ISSN 2635-1676, Nanobiotechnology Reports, 2024, Vol. 19, Suppl. 1, pp. S138–S145. © Pleiades Publishing, Ltd., 2024.

NANOMATERIALS FOR FUNCTIONAL AND STRUCTURAL PURPOSES

Synthesis of β-SiC Using Nanofibrous Carbon

Yu. L. Krutskii[a], T. S. Gudyma[a,*], A. I. Aparnev[a], A. V. Loginov[a], T. M. Krutskaya[b], A. V. Ukhina[c], N. Yu. Cherkasova[a], O. V. Netskina[d,e], and E. A. Maximovskiy[f]

[a] *Novosibirsk State Technical University, Novosibirsk, 630073 Russia*
[b] *Novosibirsk State University of Architecture and Civil Engineering (Sibstrin), Novosibirsk, 630008 Russia*
[c] *Institute of Solid State Chemistry and Mechanochemistry, Siberian Branch, Russian Academy of Sciences, Novosibirsk, 630128 Russia*
[d] *Boreskov Institute of Catalysis, Siberian Branch, Russian Academy of Sciences, Novosibirsk, 630090 Russia*
[e] *Novosibirsk State University, Novosibirsk, 630090 Russia*
[f] *Nikolaev Institute of Inorganic Chemistry, Siberian Branch, Russian Academy of Sciences, Novosibirsk, 630090 Russia*
**e-mail: gudymatan@mail.ru*

Received March 11, 2024; revised May 17, 2024; accepted May 17, 2024

Abstract—The synthesis and study of the characteristics of β-phase silicon carbide powder is carried out. The compound is obtained by combining endothermic and exothermic reactions (carbothermic reduction of silicon dioxide and synthesis from simple substances) in an induction furnace in an atmosphere of nitrogen and carbon monoxide (CO). Nanofibrous carbon (NFC) is used as the reducing agent and carbide-forming reagent. This carbon agent is obtained as a result of the decomposition of light hydrocarbons. NFC is characterized by a high specific surface area (~150 m^2/g) in comparison, for example, with carbon black (~50 m^2/g). NFC is a fairly pure material and the impurity content in it does not exceed 1 wt %. Optimization of the synthesis conditions made it possible to obtain a single-phase product: cubic silicon carbide β-SiC. The powder had an average particle size of ~4 μm and a specific surface area of 7.7–8.4 m^2/g. The resulting silicon carbide barely oxidizes when heated to 1000°C. Completion of the synthesis reaction is achieved for samples whose charge contained NFC, silicon oxide, and silicon powder in a molar ratio of 4 : 1 : 1, respectively. The optimal synthesis temperature is 1700–1900°C.

DOI: 10.1134/S2635167624602663

INTRODUCTION

In modern technology, nonmetallic refractory compounds have found wide application. They are characterized by a predominantly covalent type of bond. This is the reason for their high melting temperatures (up to 3000–3500°C), usually incongruent melting, very low values of the thermal expansion coefficient, high heat resistance, and high chemical resistance in aggressive environments. These compounds have the properties of dielectrics or semiconductors with wide band gaps, and many of them have a high thermal conductivity. The Vickers hardness of these materials varies over a wide range: from low for boron nitride in the hexagonal modification to ~50 GPa for boron carbide and chemical compounds in the boron–silicon–carbon system, one of which is silicon carbide [1].

Silicon carbide is widely used as an abrasive due to its hardness, large production volumes, and relatively low cost [2]. SiC is the main material for the production of ceramics, which are extensively employed in the space and aviation industries for manufacturing units and parts of gas turbine engines, nose cones, and the leading edges of spacecraft wings [3, 4]. SiC is used as a component in composite materials resistant to high impact loads [5, 6]. Due to their high wear resistance, SiC-based materials are used in elements of automotive braking systems [7]. Metallurgical SiC (contains 89–91 wt % SiC) is used instead of ferrosilicon in steelmaking as a deoxidizer, carburizer, and to adjust the silicon composition of the melt [1]. There is evidence that fiber-reinforced silicon carbide (SiC_f/SiC composites) can be used in nuclear reactors [8, 9]. Such composites may be promising in the manufacture of parts that operate under conditions of high abrasive action [10]. SiC-based materials may have potential applications in the field of orthopedics, including the possibility of their use to coat titanium hip prostheses [11, 12]. Silicon carbide is used as a component of refractory materials in kilns for firing ceramics [13]. Also, power semiconductor devices are created on the basis of silicon carbide [14]. It is known [15, 16], that SiC exists in two main forms: cubic with a sphalerite structure (β-SiC) and hexagonal close-packed with a wurtzite structure (α-SiC). It is believed that β-SiC is a low-temperature modification that transforms into the hexagonal modification at a temperature of about 2000°C. In [17], cubic SiC with a large surface area (~150 m^2/g) was used as a catalyst support (platinum) in the oxidation of carbon monoxide to dioxide. Also, SiC of this modification is used to obtain high-quality composite coatings during nickel and chromium plating [18]. The introduction of ultradispersed β-SiC powder into magnesium alloys in an amount of up to 5 wt % leads to an increase in the microhardness and tensile strength of the material [19]. β-SiC also proves to be an effective modifying additive in aluminum alloys [20].

There are several methods for producing silicon carbide. The industrial production of SiC is based on the carbothermic reduction of silicon dioxide:

$$SiO_2 + 3C = SiC + 2CO. \quad (1)$$

The main components of the charge are silica and petroleum coke. There is experimental evidence that the decomposition of silicon(IV) oxide leads to the formation of silicon(II) oxide and oxygen. The formation of silicon carbide occurs as a result of the interaction of silicon monoxide vapor with carbon and gaseous CO [15, 16, 21]. For this reason, the use of carbon materials with high specific surface area values is advisable for this process. Other sources of silicon dioxide and carbon can also be used in the carbothermic method. In [22] thermally expanded graphite and amorphous carbon dioxide were used. Synthesis was carried out at a temperature of 1450°C in an atmosphere of a mixture of argon and hydrogen. β-SiC nanofibers with a length of several hundred micrometers and a diameter of 30–100 nm were obtained. Data on the purity of the obtained β-SiC silicon carbide modification are not provided. Obtaining a material containing SiC is possible by the heat treatment of rice husks at 1550°C [23]. In [24] a mixture consisting of silicon dioxide and graphite, after long term (40 h) mechanical activation, was kept in a microwave oven for 5 min at 1200°C. The resulting nanopowders (particle size 10–40 nm) consisted of 98.5 wt % silicon carbide of the β-SiC modification with a small amount of α-SiC. In [25], a charge of silicon dioxide and sucrose was kept at a temperature of 1500°C for 2 h. The resulting sample consisted predominantly of aggregated β-SiC particles up to 300 nm in size with small inclusions of α-SiC. It is possible to obtain low-temperature modification SiC powder with an average particle size of 686 nm from quartz, carbon black, and phenolic resin by heat treatment in a plasma furnace for 5 min at 1800°C [26]. It was noted that increasing the synthesis temperature to 1900°C led to an increase in the yield of SiC to 98.3% and an increase in the average particle size to 1.132 μm. In [27], SiC with particle sizes from 20 to 70 nm was obtained by heating a mixture of silicon dioxide and graphite nanopowders for 1 h at 1450°C [28]. The synthesis of silicon carbide nanofibers was carried out in an induction crucible furnace at a temperature of 1400°C by the carbothermic reduction of silicon oxide with nanofibrous carbon [28]. The synthesis time was 20 min in an argon atmosphere. The diameter of the resulting SiC nanofibers was about 50–200 nm, and the length was from ten to several hundred micrometers. To scale up the process of the carbothermic synthesis of dispersed SiC powders, a method has been proposed that consists of forming a protective environment during the synthesis process. For example, in [29] the charge was placed in a graphite crucible with a lid, which, in turn, was placed in an outer crucible made of aluminum oxide. The crucible with the charge was filled with a layer of graphite powder and a layer of powdered ceramic material with a melting point above 1600°C. A protective atmosphere was formed in the outer crucible due to gaseous products (mainly CO) formed during the synthesis process [30]. A technology has been developed for producing porous ceramics using the direct carbothermic synthesis of SiC in a pressed charge of initial components (natural graphite and marshalite) [29]. To implement this technology, the batch is first pressed, then the pressed samples are subjected to heat treatment at a temperature of 1650°C and annealed at a temperature of 1550°C in air.

The synthesis of SiC from simple substances is described by the reaction

$$Si + C = SiC. \quad (2)$$

This process is characterized by a relatively low thermal efficiency (1798 kJ/kg) [31]. Therefore, the synthesis of SiC by the method of self-propagating high-temperature synthesis (SHS) can only be carried out by heating the reaction mixture [32] or as a result of mechanical activation [33]. SiC can also be obtained by the metallothermic method [34]. For instance, in [35] a mesoporous SiC powder characterized by a specific surface area of 330 m^2/g and mesoporosity of 2–10 nm was obtained by magnesiothermic synthesis using, in addition to magnesium, mesoporous silicon oxide and polyacrylamide. In [34] magnesium powder, mesoporous carbon, and zeolite were used as reagents. As a result of magnesiothermic synthesis, a SiC powder with a particle size of 10–30 nm was obtained. A special feature of this method is the need for acidic washing to remove magnesium compounds from the reaction products. It is possible to obtain SiC by vapor-phase deposition. In [36], a nanoscale SiC powder (particle size up to 10 nm) of the cubic modification was obtained from organosilicon compounds in an argon plasma flow. In [18], the production of nanoscale (61–65 nm) SiC with a main substance content of 91–93 wt % was produced upon the interaction of silica with propane-butane in a nitrogen plasma flow. Analysis of published data showed that the possibility of using nanofibrous carbon (NFC) [37] as a carbon agent for the synthesis of carbides has been relatively poorly studied [38]. It is known that through its use, highly dispersed powders of boron carbide were obtained by synthesis from sim-

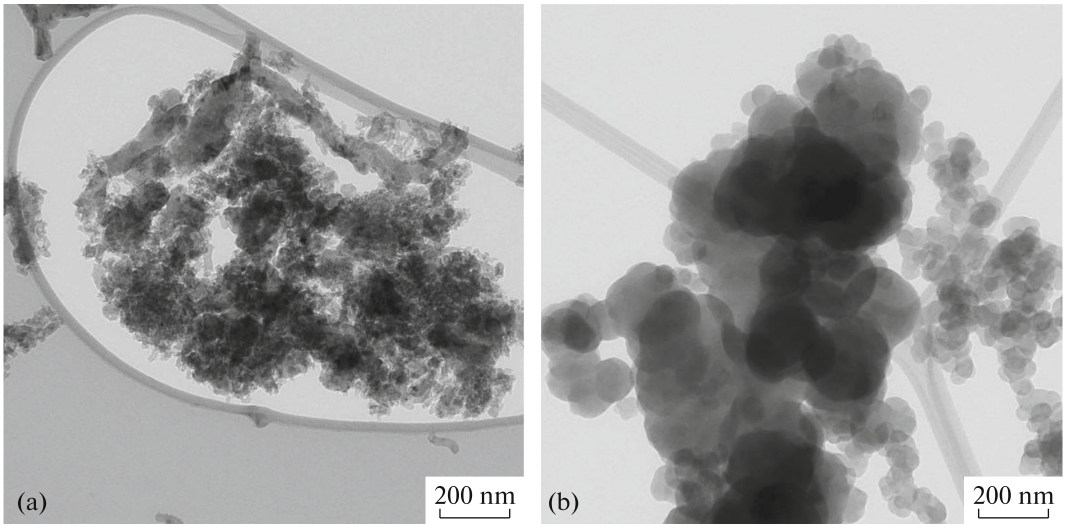

Fig. 1. High-resolution TEM images of the ground NFC (a) and carbon black (b) samples.

ple substances [39] and vanadium carbide, by the carbothermic method [40].

In this study, SiC is prepared by combining the endothermic process of carbothermic reduction and exothermic synthesis from simple substances. The charge, consisting of silicon dioxide, silicon, and NFC, is heat treated in an argon environment [38]. The disadvantages of the studied process include the implementation of synthesis in an expensive argon environment and the relatively high content of impurities in the reaction products. In this work, the synthesis of silicon carbide in a nitrogen and carbon(II) oxide atmosphere is carried out by combining these two methods using NFC.

EXPERIMENTAL

NFC with a carbon content of 99 wt % was used to carry out synthesis. The initial carbon material was represented by granules 4–8 mm in size, consisting of tightly intertwined fibers with a diameter of 30–100 nm. In addition, the NFC composition included catalyst impurities: nickel and aluminum compounds (in total less than 1 wt %). Granules of carbon material were ground in an AGO-2S planetary ball mill for 5 min with an acceleration of 15 g and a NFC-to-ball mass ratio of 1 : 15 (ball material is ZrO_2). The specific surface area of the NFC after grinding was 150 m^2/g, while the carbon black commonly used for these purposes has a specific surface area of approximately 50 m^2/g. The analysis of carbon agents by transmission electron microscopy (TEM) showed that the NFC has a more developed surface compared to carbon black (Fig. 1).

Technical silicon KR00 (GOST (State Standard) 2169-69) and amorphous silicon oxide OSCh 7-3 (Technical Specification 6-09-4574-85) were also used for synthesis. The silicon was pre-ground in the AGO-2S planetary ball mill for 5 min with an acceleration of 20*g* with silicon-to-ball mass ratio of 1 : 30. All reagents were pre-dried at 100°C and then sieved through a sieve with a cell diameter of 100 μm. The initial powder mixtures were prepared in accordance with the stoichiometry of reactions (1) and (2), after which the indicated compositions were mixed in molar ratios of 0.25 : 0.75 for charge 1, 0.50 : 0.50 for charge 2, and 0.75 : 0.25 for charge 3. Thus, the molar ratio of components for charges 1, 2, and 3 was as follows: $SiO_2 : Si : C = 1 : 3 : 6$; $SiO_2 : Si : C = 1 : 1 : 4$; $SiO_2 : Si : C = 3 : 1 : 10$, respectively.

Heat treatment of the specified compositions was carried out using a VCh-25 AV induction furnace. Synthesis was carried out in graphite crucibles installed in a reactor made of quartz glass in air. The temperature in the reactor during synthesis was determined using an optical pyrometer. After completion of the synthesis process, the reactor was cooled to room temperature, and then the reaction products were extracted. When the crucible was heated, it was partially oxidized by atmospheric oxygen, as a result of which the gas environment during the synthesis of silicon carbide at a temperature of 1700–1900°C consisted of nitrogen and carbon monoxide. Therefore, the partial pressure of CO in its mixture with nitrogen was lower than atmospheric pressure. In accordance with the methodology in [41] the change in the Gibbs free energy for reaction (1) was calculated at different pressures of carbon monoxide. It was established that at CO pressures of 0.1, 0.01, 0.001, and 0.0001 MPa, the value of the free energy becomes negative at temperatures of 1437, 1269, 1132, and 1017°C, respectively. However, the process of complete conversion of reagents into products will occur at significantly higher temperatures. In this work, experiments on the

Table 1. Temperature of SiC powder synthesis depending on the composition of the charge

Charge	Sample	*T*, °C	Estimated mass loss, wt %	Experimental mass loss, wt %
1	SiC II	1700	25.9	17.3
	SiC I-II	1900		21.0
2	SiC II-I	1700	41.2	41.6
	SiC II-II	1900		41.9
3	SiC III-I	1700	51.2	31.9
	SiC III-II	1900		37.8

synthesis of silicon carbide were carried out (taking into account the information presented in [38]) at temperatures of 1700 and 1900°C. Taking into account the exothermic nature of reaction (2), the process temperature will be higher, but heat losses from the crucible surface (mainly due to radiation) should be taken into account. At such relatively low temperatures, the formation of cubic silicon carbide (β-SiC) is most likely. Homogenization of the charge components was carried out using an AGO-2S planetary ball mill for 5 min at an acceleration of 20*g*. The charge-to-ball mass ratio of was 4 : 75. The charge was subjected to heat treatment for 20 min. Research [40], conducted earlier, showed that this duration of synthesis is optimal for a charge weighing 20 g.

To assess the degree of completion of the reaction, the method of weighing and comparing experimental data with theoretical data was used. The reaction products were analyzed by X-ray diffraction using an ARL X'TRA diffractometer with a copper X-ray tube as the X-ray source. To identify the phase composition, the PDF4+ software package and the ICDD PDF4+ electronic database were used. The polytypic composition was assessed in accordance with the methodology in [42]. The morphology and elemental composition of the samples were studied using an EVO50 scanning electron microscope (SEM) with an X-Act attachment for energy-dispersive microanalysis. The particle size was determined using a BA Instruments MicroSizer 201 laser particle analyzer. The textural characteristics of the samples were investigated by isothermal low-temperature nitrogen adsorption and desorption at 77 K using a Quantochrom NOVA 2200e instrument, and the specific surface area was calculated using the Brunauer–Emmett–Teller method. The crystallite size in the silicon carbide phase was determined using the Scherrer equation taking into account instrumental broadening. The thermal-oxidative stability of the powders was studied using a NETZSCH STA 449C Jupiter device in a synthetic air atmosphere at a heating rate of 10 K/min.

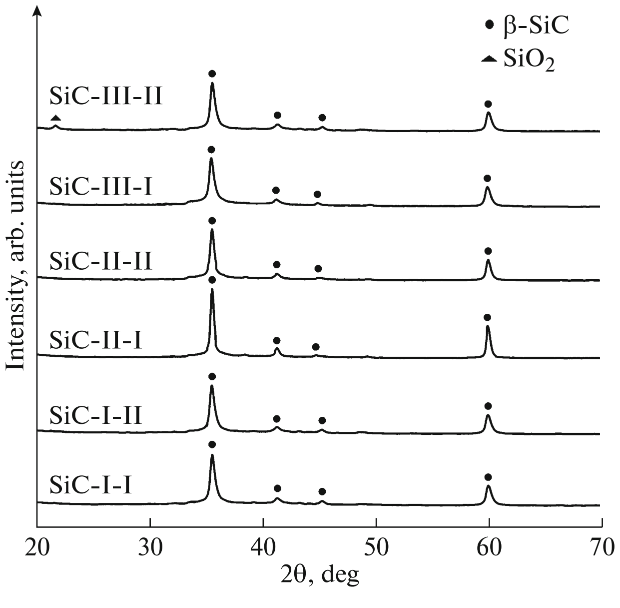

Fig. 2. Diffraction patterns of the samples.

RESULTS AND DISCUSSION

Table 1 shows the conditions for carrying out the synthesis of materials depending on the composition of the charge, as well as data on the mass loss of the charge as a result of heat treatment. For some samples (SiC II-I and SiC II-II) a slight excess of mass loss was recorded compared to the calculated values. The deviation is probably due to the partial loss of SiO_2 in the form of volatile silicon monoxide SiO.

The results of X-ray phase analysis of the samples are shown in Fig. 2.

Analysis of the diffraction patterns showed that all samples consist predominantly of cubic SiC. Minor peaks in the region of 33°–35° and 38°–39° in the diffraction patterns may indicate the presence of an admixture of 6H and 4H polytypes of hexagonal silicon carbide (α-SiC). Also, the presence of minor unidentifiable peaks in the region of 43°–45° may indicate the presence of impurities introduced from reagents. The results obtained are apparently reliable, since heat treatment of the charges was carried out at relatively low temperatures (1700 and 1900°C).

The results of energy-dispersive analysis showed the presence of oxygen in all samples (Table 2). This indicates the presence of unreacted SiO_2 in the powders. Nitrogen was not detected in any of the samples.

The ratio of Si and C closest to the theoretical one (1 : 1), was typical for SiC II-I and SiC II-II samples. This indicates that the synthesis reaction proceeds most completely in this case. All samples showed a slight upward deviation from the stated carbon content ratio, indicating the presence of unreacted NFC.

Table 2. Energy-dispersive analysis data (at %)

Element	Sample					
	SiC II	SiC I-II	SiC II-I	SiC II-II	SiC III-I	SiC III-II
C	52.5	51.5	50.6	50.3	56.4	55.1
O	3.5	3.7	1.3	0.1	7.1	9.4
Si	42.8	43.8	47.2	48.8	35.2	34.2
Catalyst metals	1.2	1.0	0.9	0.8	1.3	1.3

SEM images of the samples are shown in Fig. 3. The particles are predominantly aggregated. Histograms of the particle size distribution are shown in Fig. 4.

In accordance with the methodology given in [43], the average particle/aggregate sizes of the powders, and the standard deviation and skewness coefficient of the histograms were calculated (Table 3).

In the standard deviation range of 2.0–4.0 μm, particles/aggregates are “poorly sorted.” The particle distribution is considered symmetrical in the range of the skewness coefficient from –0.43 to +0.43.

The specific surface area values of the SiC I-I, SiC I-II, SiC II-I, SiC II-II, SiC III-I, and SiC III-II samples were 9.4, 9.1, 8.4, 7.7, 10.5, and 7.9 m^2/g, respectively. The higher values of the specific surface area of the SiC I-I, Si I-II, SiC III-I, and SiC III-II samples are apparently associated with the increased content of free carbon impurity in them.

Determination of the average crystallite size L was performed based on X-ray phase analysis data using the Scherrer equation with the help of the Expert software:

$$L = \frac{k\lambda}{B\cos(\theta)}, \tag{3}$$

where k is the Scherrer constant, $k = 0.94$; λ is the radiation wavelength, $\lambda = 0.15406$ nm; B is the peak width at half height, rad; and θ is the Bragg angle.

The crystallite sizes of the SiC I-I, SiC I-II, SiC II-I, SiC II-II, SiC III-I, and SiC III-II samples were 30, 28, 29, 30, 31, and 32 nm, respectively. Thus, the dependence of these values on the heat-treatment temperature and charge compositions was not detected. In addition, the indicated crystallite size is close to the diameter of the carbon nanofibers used. This may be experimental confirmation of the synthesis occurring through the formation of gaseous silicon monoxide and pseudomorphs of carbon.

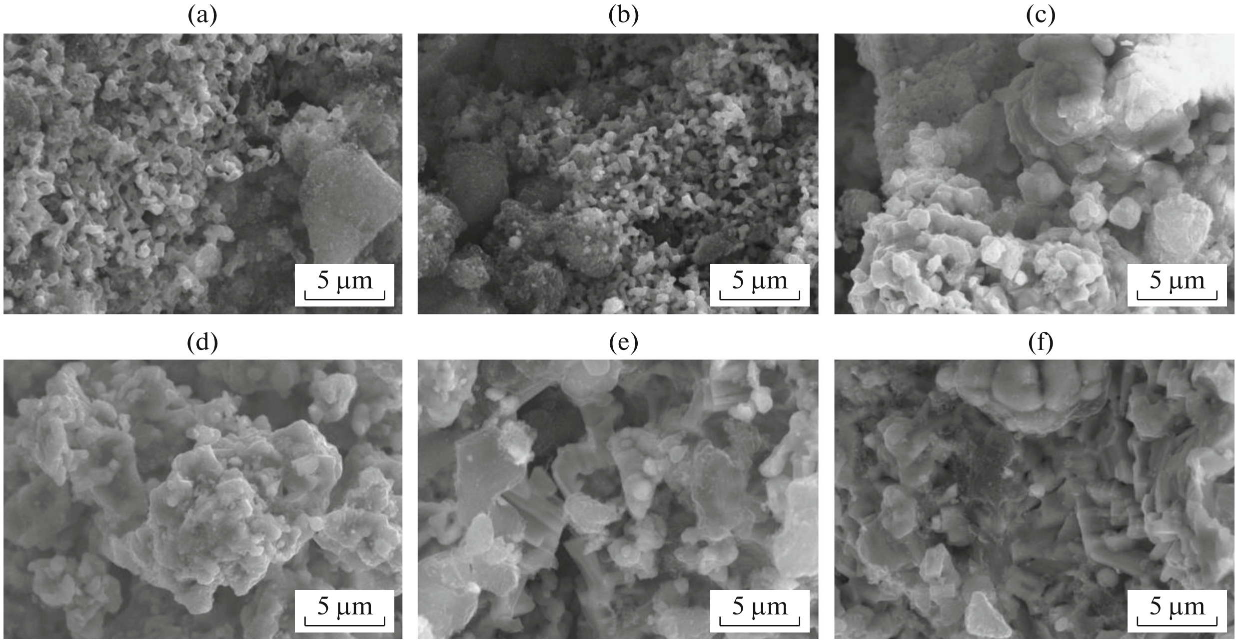

Fig. 3. SEM images of the samples: (a) SiC I-I, (b) SiC I-II, (c) SiC II-I, (d) SiC II-II, (e) SiC III-I, (f) SiC III-II.

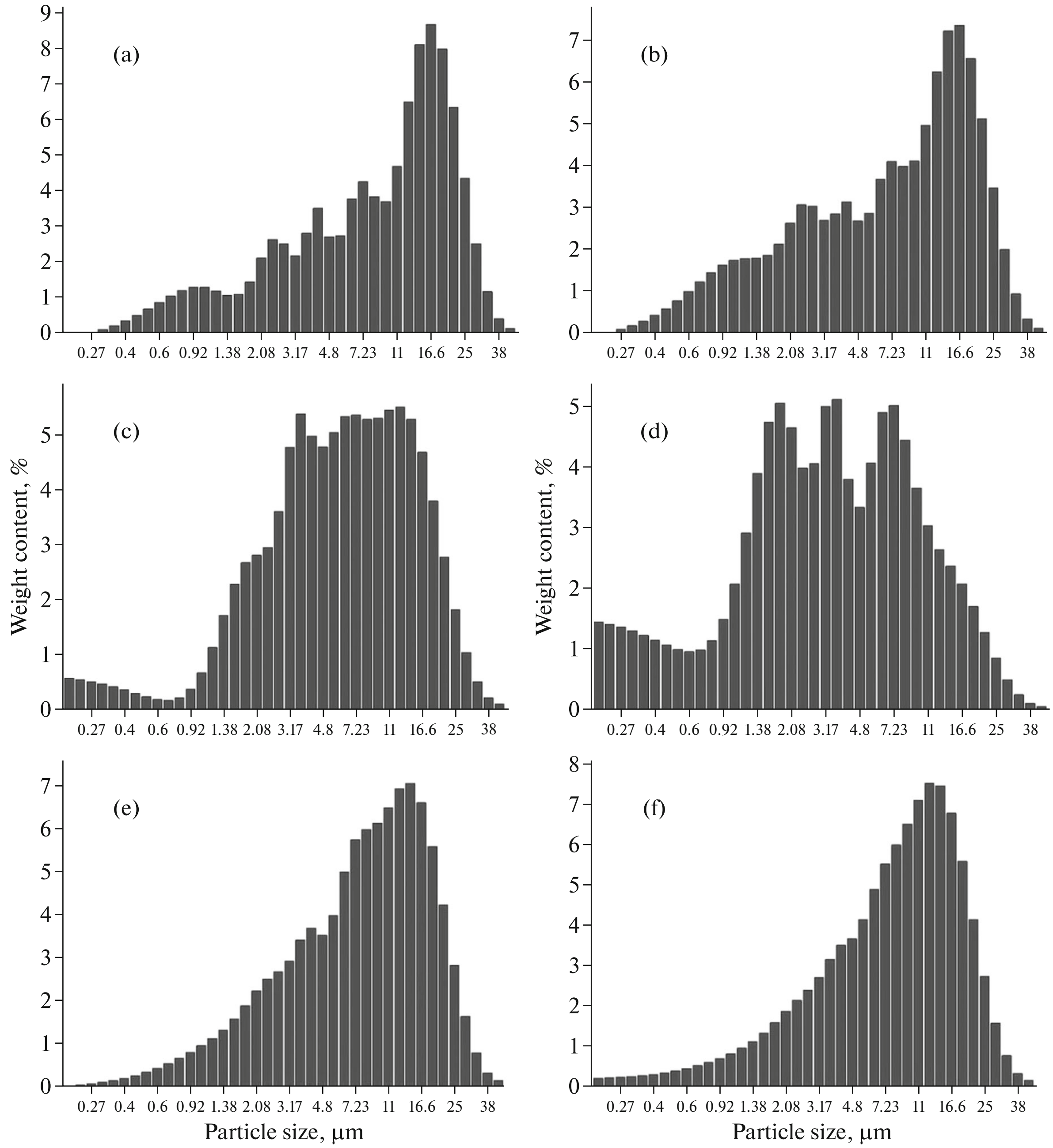

Fig. 4. Histograms of particle size distribution: (a) SiC I-I, (b) SiC I-II, (c) SiC II-I, (d) SiC II-II, (e) SiC III-I, (f) SiC III-II.

The results of the mass loss data, as well as the X-ray phase and energy-dispersive analyses, showed that the most complete course of the synthesis reaction was achieved for the samples obtained using charges 2 (SiC II-I and SiC II-II). Therefore, thermal studies were carried out on them. The oxidation of silicon carbide at high temperatures proceeds in accordance with the thermodynamically most probable reaction [16, 44]:

$$SiC + 2O_2 = SiO_2 + CO_2. \tag{4}$$

With the complete oxidation of silicon carbide in accordance with reaction (4), the mass increase will be 50%. According to the data of synchronous thermal analysis, the mass increase of the SiC II-I sample begins at approximately 550°C and, upon reaching 1000°C, it is 2.7%. This indicates insignificant oxidation of the sample under the specified conditions and high oxidative stability of the material. For the SiC II-II sample, starting from approximately the same temperature, there is a mass loss (2.6%) with an accompanying exothermic effect in the temperature range of

Table 3. Particle-size analysis results

Sample	Average particle/aggregate size, μm	Standard deviation, μm	Indicator asymmetries
SiC II	8.1	2.87	–0.35
SiC I-II	7.9	3.03	–0.30
SiC II-I	3.5	3.18	–0.20
SiC II-II	4.3	2.75	–0.22
SiC III-I	7.6	2.46	–0.23
SiC II-II	7.8	2.56	–0.33

550–680°C. This may be due to the oxidation of unreacted carbon, the content of which is probably below the detection limit of the diffractometer. Thus, when heating SiC II-I and SiC II-II samples in an oxidizing environment to 1000°C, no significant changes in the mass of the sample occur, i.e., the resulting silicon carbide has high corrosion resistance.

CONCLUSIONS

The synthesis of highly dispersed SiC powder by combining carbothermic reduction and synthesis from simple substances has been investigated. The results of the experiments showed that the optimal molar ratio of reagents $SiO_2 : Si : C$ is 1 : 1 : 4 at a synthesis temperature of 1700–1900°C in a nitrogen and carbon monoxide(II) atmosphere. The impurity content in the obtained materials was at a level of approximately 2 wt %. According to SEM data, it was established that the powder particles are characterized by the presence of aggregates. The average particle size was 3.5–4.3 μm, and the specific-surface-area values were in the range of 7.7–8.4 m^2/g. Silicon carbide samples obtained under optimal conditions barely underwent oxidation in a synthetic air environment when heated to 1000°C. It was shown that by combining endothermic and exothermic reactions of carbide formation, it is possible to obtain a highly dispersed unground powder of cubic silicon carbide (β-SiC) with a low impurity content.

FUNDING

The study was performed in accordance with the state order of the Ministry of Science and Higher Education of the Russian Federation (code FSUN-2023-0008).

CONFLICT OF INTEREST

The authors of this work declare that they have no conflicts of interest.

REFERENCES

1. O. A. Ageev, A. E. Belyaev, N. S. Boltovets, et al., *Silicon Carbide: Technology, Properties, Application* (ISMA, Kharkiv, 2010) [in Russian].
2. A. N. Porada and M. I. Gasik, *Electrothermy of Inorganic Materials* (Metallurgiya, Moscow, 1990) [in Russian].
3. F. Monteverde, Corrosion Sci. **53**, 922 (2011). https://doi.org/10.1016/j.corsci.2010.11.018
4. O. N. Grigoryev, Poroshkovaya Metallurg., Nos. 11–12, 100 (2012).
5. A. P. Garshin, V. I. Kulik, and A. S. Nilov, Novye Ogneupory, No. 4, 53 (2016). https://doi.org/10.17073/1683-4518-2016-4-53-67
6. I. Yu. Kelina, V. V. Lensky, N. A. Golubeva, et al., Ogneupory Tekh. Keramika, Nos. 1–2, 17 (2010).
7. W. Krenkel and F. Berndt, Mater. Sci. Eng., A **412**, 177 (2005). https://doi.org/10.1016/j.msea.2005.08.204
8. B. Riccardi, L. Giancarli, A. Hasegawa, et al., J. Nucl. Mater. **329**, 56 (2004). https://doi.org/10.1016/j.jnucmat.2004.04.002
9. Y. Katoh, L. L. Snead, I. Szlufarska, et al., Curr. Opin. Solid State Mater. Sci. **16**, 143 (2012). https://doi.org/10.1016/j.cossms.2012.03.005
10. P. Aspenberg, A. Anttila, Y. T. Konttinen, et al., Biomaterials **17**, 807 (1996). https://doi.org/10.1016/0142-9612(96)81418-9
11. L. Nordsletten, A. Hogasen, Y. T. Konttinen, et al., Biomaterials **17**, 1521 (1996). https://doi.org/10.1016/0142-9612(96)89777-8
12. E. A. Gerasimova, L. Ya. Guzman, and G. E. Karas', Refractories **31**, 208 (1990).
13. M. G. Frolova, Yu. F. Kargin, A. S. Lysenkov, et al., Inorg. Mater. **56**, 987 (2020). https://doi.org/10.1134/S0020168520090058
14. E. M. Geifman, I. V. Grekhov, G. Yu. Kamenets, Nanoindustriya **13**, 278 (2020). https://doi.org/10.22184/1993-8578.2020.13.4s.278.280
15. V. A. Ershov, *Electrothermal Processes of Chemical Technology* (Khimiya, Leningrad, 1984) [in Russian].
16. T. Ya. Kosolapova, T. V. Andreeva, and T. S. Bartnitskaya, *Non-Metallic Refractory Compounds* (Metallurgiya, Moscow, 1985) [in Russian].
17. N. N. Vershinin, V. A. Bakaev, V. I. Berestenko, et al., High Energy Chem **51**, 46–50 (2017). https://doi.org/10.1134/S0018143916060199
18. O. A. Polyakh and V. V. Rudneva, *Plasma Metallurgical Production of Silicon Carbide for Composite Nickel Plating and Chromium Plating* (Nauka, Moscow, 2006) [in Russian].
19. A. S. Lebedev, Candidate's Dissertation in Chemistry (Yuzhno-Ural'sk. Gos. Univ, Chelyabinsk, 2000).
20. A. S. Lebedev, V. E. Eremyshev, and A. V. Suzdal'tsev, Elektrometallurgiya, No. 1, 17 (2020).
21. A. S. Lebedev, A. V. Suzdal'tsev, and V. N. Anfilogov, Neorg. Mater. **56**, 22 (2020). https://doi.org/10.31857/S0002337X20010091

22. H. J. Hwang, K.-J. Lee, Y.-T. An, et al., Mater. Chem. Phys. **134**, 13 (2012). https://doi.org/10.1016/j.matchemphys.2012.02.056
23. G. T. Adylov, Sh. A. Faiziev, and M. S. Paizullakhanov, Tech. Phys. Lett. **29**, 221–223 (2003). https://doi.org/10.1134/1.1565639
24. B. M. Moshtaghioun, R. Poyato, F. L. Cumbrera, et al., J. Eur. Ceram. Soc. **32**, 1787 (2012). https://doi.org/10.1016/j.jeurceramsoc.2011.12.021
25. L. G. Ceballos-Mendivil, R. E. Cabanillas-Lopez, J. C. Tanori-Codova, et al., Sol. Energy **116**, 238 (2015). https://doi.org/10.1016/j.solener.2015.04.006
26. F. Wang, D. Xiang, Y. Wang, et al., Ceram. Int. **43**, 4970 (2017). https://doi.org/10.1016/j.ceramint.2017.01.003
27. B. M. Moshtaghioun, A. Monshi, M. H. Abbasi, et al., Int. J. Refract. Met. Hard Mater. **29**, 645 (2011). https://doi.org/10.1016/j.ijrmhm.2011.04.009
28. X. Luo, W. Ma, Y. Zhou, et al., Nanoscale Res. Lett. **5**, 252 (2010). https://doi.org/10.1007/s11671-009-9474-8
29. A. S. Lebedev, V. N. Anfilogov, and I. A. Blinov, **468**, 156–158 (2016). https://doi.org/10.1134/S0012500816050050
30. V. N. Anfilogov and A. S. Lebedev, RU Patent No. 2537616 (2015).
31. T. Ya. Kosolapova, *Properties, Production, and Application of Refractory Compounds* (Metallurgiya, Moscow, 1986) [in Russian].
32. D. Kata, J. Lis, R. Pampuch, et al., Int. J. Self-propagating High-Temp. Synth. **7**, 475 (1998).
33. H.-B. Jin, J.-T. Li, M.-S. Cao, et al., Powd. Techn. **196**, 229 (2009). https://doi.org/10.1016/j.powtec.2009.07.016
34. B. Hosseini, A. A. Nourbacksh, and K. J. D. MacKenzie, Ceram. Int. **41**, 8809 (2015). https://doi.org/10.1016/j.ceramint.2015.03.107
35. Z. Saeedifar, A. A. Nourbacksh, R. J. Kalbasi, et al., J. Mater. Sci. Techn. **29**, 255 (2013).
36. C. Czosnek, M. Bucko, J. F. Janik, et al., Mater. Res. Bull. **63**, 164 (2015). https://doi.org/10.1016/j.materresbull.2014.12.003
37. G. G. Kuvshinov, Yu. L. Mogilnykh, D. G. Kuvshinov, et al., Carbon **37**, 1239 (1999). https://doi.org/10.1016/S0008-6223(98)00320-0
38. T. S. Kvashina, Yu. L. Krutskiy, and N. Yu. Cherkasova, Dokl. Akad. Nauk Vyssh. Shkoly **37**, 80 (2017). https://doi.org/10.17212/1727-2769-2017-4-80-90
39. R. G. Shumilova and T. Ya. Kosolapova, Poroshkovaya Metallurg., No. 11, 906 (1968).
40. Yu. L. Krutskiy, A G Tyurin, M. V. Popov, et al., Steel Transl. **48**, 207 (2018). https://doi.org/10.3103/S096709121804006X
41. L. P. Vladimirov, *Thermodynamic Calculations of the Equilibrium of Metallurgical Reactions* (Metallurgiya, Moscow, 1970) [in Russian].
42. J. Ruska, L. J. Gauckler, J. L. Lorenz et al., J. Mat. Sci. **14**, 2013 (1979). https://doi.org/10.1007/BF00551044
43. S. J. Blott and K. Pye, Earth Surf. Processes Landforms **26**, 1237 (2001). https://doi.org/10.1002/esp.261
44. D. M. Benevolensky, A. I. Dus', and S. M. Movnin, Izv. St. Petersburg Gos. Elektrotekh. Univ., No. 10, 5 (2018).